What's behind 68Ga-PSMA-11 Uptake in Primary Prostate Cancer PET? Investigation of Histopathological Parameters and Immunohistochemical PSMA Expression Patterns.

Jan H. Rüschoff (janhendrik.rueschoff@usz.ch)
Department of Pathology and Molecular Pathology, University Hospital Zurich https://orcid.org/0000-0002-1936-6606

Daniela A. Ferraro
Department of Nuclear Medicine, University Hospital Zurich

Urs J. Muehlematter
Department of Nuclear Medicine, University Hospital Zurich

Thomas Hermanns
Department of Urology, University Hospital Zurich

Ann-Katrin Rodewald
Department of Pathology and Molecular Pathology, University Hospital Zurich

Holger Moch
Department of Pathology and Molecular Pathology, University Hospital Zurich

Daniel Eberli
Department of Urology, University Hospital Zurich

Irene A. Burger
Department of Nuclear Medicine, University Hospital Zurich

Niels J. Rupp
Department of Pathology and Molecular Pathology

Research Article

Keywords: Prostatic Neoplasms, Immunohistochemistry, Glutamate Carboxypeptidase II, Positron-Emission Tomography, Neoplasm Staging

Posted Date: April 30th, 2021

DOI: https://doi.org/10.21203/rs.3.rs-461507/v1

Version of Record: A version of this preprint was published at European Journal of Nuclear Medicine and Molecular Imaging on August 13th, 2021. See the published version at https://doi.org/10.1007/s00259-021-05501-1.

Abstract

Purpose: Prostate specific membrane antigen (PSMA-) PET has become a promising tool in staging and restaging of prostate carcinoma (PCa). However, specific primary tumour features might impact accuracy of PSMA-PET for PCa detection. We investigated histopathological parameters and immunohistochemical PSMA expression patterns on radical prostatectomy (RPE) specimens and correlated them to the corresponding ^{68}Ga-PSMA-11-PET examinations.

Methods: RPE specimen of 62 patients with preoperative ^{68}Ga-PSMA-11-PET between 2016 and 2018 were analyzed. WHO/ISUP grade groups, growth pattern (expansive vs. infiltrative), tumour area and diameter as well as immunhistochemical PSMA heterogeneity, intensity and negative tumour area ($PSMA_{\%neg}$) were correlated with spatially corresponding SUV_{max} on ^{68}Ga-PSMA-11-PET in a multidisciplinary analysis.

Results: All tumours showed medium to strong membranous (2-3+) and weak to strong cytoplasmic (1-3+) PSMA expression. Heterogeneously expressed PSMA was found in 38 cases (61%). Twenty-five cases (40%) showed at least 5% and up to 80% $PSMA_{\%neg}$. $PSMA_{\%neg}$, infiltrative growth pattern, smaller tumour area and diameter and WHO/ISUP grade group 2 significantly correlated with lower SUV_{max} values. A ROC curve analysis revealed 20% $PSMA_{\%neg}$ as an optimal cutoff with the highest sensitivity and specificity (89% and 86%, AUC 0.923) for a negative PSMA-PET scan. A multiple logistic regression model revealed tumoural $PSMA_{\%neg}$ ($p<0.01$, OR=9.629) and growth pattern (p=0.0497, OR=306.537) as significant predictors for a negative PSMA-PET scan.

Conclusions: We describe $PSMA_{\%neg}$, infiltrative growth pattern, smaller tumour size and WHO/ISUP grade group 2 as parameters associated with a lower ^{68}Ga-PSMA-11 uptake in prostate cancer. These findings can serve as fundament for future biopsy-based biomarker development to enable an individualized, tumour-adapted imaging approach.

Background

Prostate specific membrane antigen (PSMA) is a 100 kDa type II transmembrane protein (1) and is commonly upregulated in prostate carcinoma (PCa) (2). PSMA expression in PCa correlates with higher tumour grade (Gleason Score) and is an independent predictor for PCa progression (3-5). Positron emission tomography (PET) targeting PSMA linked to either ^{68}Ga or ^{18}F has changed imaging approaches for biochemical recurrence and can detect recurrence even on low PSA-levels (6) or after focal therapy (7). Additionally, first prospective studies confirmed an improved PCa staging (8) with focus on detection of nodal or distant disease. Recent data showed improved accuracy for local PCa extension (9, 10), and PCa detection in combination with magnetic resonance imaging (MRI) (11, 12). It has been suggested, that specific prostate cancer tissue features influence PSMA tracer accumulation. About 10% of PCa lack PSMA uptake and cannot be detected by PSMA-PET (13, 14). In single prostate cancer

patients, invisible PCa on multiparametric MRI (mpMRI) but positive ^{68}PSMA-11-PET has been reported (15). Heterogeneous PSMA expression has been particularly described in metastatic PCa (16), and in PCa with DNA repair defects (17). It has also been shown that the central zone of the prostate can show false positivity in ^{68}PSMA-11-PET (18). Furthermore, some reports on PSMA-PET positive lesions that correspond to normal prostatic tissue with increased PSMA expression exist (19). Only one study correlated immunohistochemical PSMA expression in primary tumours of RPE with corresponding PSMA-PET accumulation, yet (20). Exact correlation of immunohistochemical PSMA expression patterns in primary tumours of RPE with corresponding PSMA-PET accumulation is mandatory to improve the quality of ^{68}PSMA-11-PET interpretation and to pave the way for optimal molecular imaging in the future.

The aim of this study was to investigate and colocalize immunohistochemical PSMA expression patterns and histopathological features in patients with a pretherapeutic ^{68}PSMA-11-PET followed by radical prostatectomy to identify tumour characteristics that are associated with low SUV_{max} values on PSMA-PET scans.

Materials And Methods

Study population

This study included consecutive patients who underwent staging with ^{68}Ga-PSMA-11-PET for newly diagnosed intermediate or high-risk prostate cancer at the University Hospital Zurich from April 2016 to May 2018. All patients with no radical prostatectomy (RPE) specimen available were excluded. The local ethics committee approved the study protocol (BASEC Nr. 2018–01284) and all patients gave a general written informed consent for use of their data. Relevant clinico-pathological characteristics such as patients' age at the time of operation, tumour stage and (modified) Gleason Score respective WHO/ISUP prognostic grade group were collected.

Histopathological parameters and Immunohistochemistry

Sixty-two formalin-fixed, paraffin-embedded (FFPE) RPE specimen were evaluated on 2 µm hematoxylin & eosin (H&E) stained sections. One representative slide from the RPE specimen was chosen for further investigation, harbouring the largest area of tumour and therefore defining the dominant tumour lesion.

Staging and grading were done according to the WHO/ISUP/UICC guidelines (21, 22). Separate grading of the dominant tumour lesion was done and used for further correlation analysis. The tumour area and maximum diameter on each slide were measured digitally. Very small carcinoma lesions (maximum diameter < 5 mm) were excluded from statistical analysis because of a natural resolution limit of PSMA-PET scans due to partial-volume effects (23).

A newly developed type of growth pattern (infiltrative vs. expansive) of each prostate cancer lesion was determined. We defined infiltrative growth as entrapped benign glands within the carcinoma complexes. An expansive growth pattern showed a tumour infiltration of pure carcinoma glands (without intermingled benign glands) within an area of at least 3 circles of 5 mm^2 (radius 1.26 mm).

International Society of Urologic Pathology (ISUP) and World Health Organisation (WHO) guidelines, according to WHO/ISUP 2014 guidelines according to WHO/ISUP 2014 guidelines

Immunohistochemical staining for PSMA (DAKO, M3620, clone 3E6, 1:25) was performed as described previously (24). The predominant PSMA expression patterns were visually quantified using a four-tiered system (0 = negative, 1+ = weak, 2+ = moderate, 3+ = strong) for both membranous and cytoplasmic PSMA expression by two board certified, experienced genito-urinary pathologists (J.H.R, N.J.R.). Examples of expression patterns are shown in Fig. 1. Furthermore, tumour areas without PSMA expression were quantified in steps of 5%, 10% and further 10% increments in relation to the total tumour area, as percentage PSMA-negative tumour area ($PSMA_{\%neg}$) as a consent of both pathologists. Heterogeneity was defined by differences in the staining pattern of at least 5% of the representative tumour slide (Fig. 2).

Slides were digitalized (Nanozoomer NDP digital slide scanner C9600-12) using the Hamamatsu NDP.view 2.8.24 Software.

Imaging

Patients underwent clinical routine ^{68}Ga-PSMA-11-PET/computed tomography (CT) on a Discovery VCT 690 PET/CT (GE Healthcare, Waukesha, WI, USA) or on a Discovery MI PET/CT (GE Healthcare, Waukesha, WI, USA) or ^{68}Ga-PSMA-11-PET/MRI (SIGNA PET/MR, GE Healthcare, Waukesha, WI, USA) after a single injection of ^{68}Ga-PSMA-11 (mean dose ± standard deviation (SD) 130 ± 18 MBq, range 81-171 MBq). The institutional protocol is in agreement with the EANM and SNMMI procedure guidelines (25). Details are given in the supplements.

Imaging analysis

The acquired PET/CT and PET/MR images were analysed in a dedicated review workstation (Advantage Workstation, Version 4.6 or 4.7, GE Healthcare), which enables the review of the PET and the CT or MR images side by side and in fused mode. Every patient was discussed in a multidisciplinary set up including a pathologist and a nuclear medicine physician and radiologist with the selected pathology slide available alongside with the PET data. The corresponding area on PET images with the dominant tumour lesion was identified and PSMA uptake quantified using the maximum standardized uptake value (SUV_{max}). There is a wide range of proposed cutoffs to detect significant prostate cancer from SUV_{max} 3.15 (20) to up to SUV_{max} 9.1 (26). For visual identification an clear uptake above background might be

more efficient than a absolute cutoff, and given that there were no lesions in the central zone in our cohort, and to select clear positive lesions we decided to take a PSMA uptake of $SUV_{max} \geq 5$ as definition of PSMA-PET positivity (18).

An additional analysis for $SUV_{max} \geq 4$ is given in the supplements, to rule out a systematic underestimation. For the correlation between immunhistochemical (IHC)-parameters and PET quantification the spatial resolution of the PET scanners was taken into account. Therefore, a tumour diameter of 5 mm or more on histology was considered necessary for accurate quantification of PSMA-accumulation limiting the impact of partial-volume effect (23).

Correlation of histopathological and immunohistochemical parameters with SUV_{max} values

Correlations between histological parameters, immunhistochemical PSMA expression patterns and SUV_{max} values were calculated using Mann-Whitney U test, Kruskal–Wallis test and Pearson's correlation. An optimal cutoff for $PSMA_{\%neg}$ was determined using Receiver operating characteristic (ROC) analysis. We investigated the association between a combination of histological parameters and immunhistochemical PSMA expression patterns with a negative PSMA-PET scan using a multiple logistic regression analysis.

Statistical analysis

Normal distribution was tested using the Kolmogorov–Smirnov test. Comparisons were calculated with Mann-Whitney U test for binary variables and Kruskal–Wallis test for multiple variables. Correlations were done using bivariate Pearson's correlation. Discrimination was evaluated using area under the receiver operating characteristic (ROC) curve (AUC). The variables entered in the multiple logistic regression analysis were selected by univariable logistic regression with a p-value cut-off point of 0.05. For the logistic regression analyses ordinal variables were treated as continuous. Multicollinearity was assessed using Variable Inflation Factors (VIF). Two-sided p values < 0.05 were considered statistically significant. Correlations and ROC curve analysis were performed using SPSS Version 26 (IBM, Armonk, New York, USA). Logistic regression analyses were performed using R (R version 4.0.2; R Foundation for Statistical computing, Vienna, Austria). Graphs were generated using GraphPad Prism v8.

Results

Study population

^{68}Ga-PSMA-11-PET scans from 137 patients were available. Patients were excluded because of missing informed consent, treatment before PSMA-PET scan, missing clinical information and/or unavailability of

a RPE specimen. A total number of 62 patients were included in this study (Fig. 3). Clinico-pathological characteristics are shown in Tab. 1. Interval between ^{68}Ga-PSMA-11-PET and surgery ranged from one day to 6 months.

Table 1

Clinicopathological characteristics of the study cohort (n=62)

	n/mean	%/SD
Age (years)	63.98	±6.06
pT stadium	pT2a (n=2)	3.2%
	pT2b (n=2)	3.2%
	pT2c (n = 39)	62.9%
	pT3a (n = 11)	17.7%
	pT3b (n= 8)	12.9%
WHO/ISUP grade groups	Group 2: 3+4 (n=5)	8.1%
	Group 3: 4+3 (n=23)	37.1%
	Group 4: 4+4 (n=21)	33.9%
	Group 5: 4+5 (n=13)	21%
Tumour area (mm^2)	84.3 mm^2	+/- 63.5 mm^2
Tumour diameter (mm)	13.9 mm	+/- 6.0 mm

Histopathological parameters

The dominant tumour lesions showed WHO/ISUP grade groups ranging from 2 to 5 (Tab. 1). The tumour area ranged from 1.4 to 265 mm^2 (mean 84.3 +/- 63.5 mm^2), and maximum diameter was recorded from 2 to 25.7 mm (mean 13.9 +/- 6.0 mm). Four lesions were smaller than 5 mm and were excluded for correlation analysis between histology pattern and PSMA-PET uptake. An infiltrative growth pattern of the dominant tumour was seen in 33 of 62 (53.2%) cases, whereas an expansive pattern occured in 29 of 62 (46.8%) cases (Fig. 4). No significant correlation between growth pattern and WHO/ISUP grade group or pT stage was observed (each $p>0.05$, Mann-Whitney U test). Larger tumour area and higher maximum diameter were significantly correlated with expansive growth pattern (each $p<0.05$, Mann-Whitney U test). Higher WHO/ISUP grade group showed a significant association with higher pT stage ($p<0.01$, Pearson's correlation).

Immunohistochemistry

PSMA expression was noted in all 62 (100%) prostate adenocarcinoma specimen with a range from medium to strong membranous (2+ to 3+) and weak to strong (1+ to 3+) cytoplasmic expression (Fig. 2). No case with isolated cytoplasmic without membranous staining was observed. Intratumoural heterogeneity of PSMA expression could be observed in 38 of 62 cases (61%). Twenty-five cases (40%) showed areas completely negative for PSMA comprising 5% to 80% of the tumour area ($PSMA_{\%neg}$, Fig. 3).

Imaging

SUV_{max} values ranged from 3.1 to 48.4 (mean 14.96 +/- 10.8). Considering $SUV_{max} \geq 5$ as the definition for PET positivity and excluding lesions smaller than 5 mm on histopathology, 49 of 58 scans (84.5%) were positive, and 9 of 58 (15.5%) negative. Of the four lesions smaller than 5 mm two had a SUVmax ≥ 5.

Correlation of histopathological parameters and Immunohistochemistry with SUV_{max} values

The presence of PSMA negative tumour areas ($PSMA_{\%neg}$ between 5% to 80%) was significantly associated with lower SUV_{max} values (mean SUV_{max} 19.24 ± 11.1 vs. 8.89 ± 6.8, $p<0.01$, Mann-Whitney U test).

We performed ROC curve analysis showing the optimal cutoff to be $PSMA_{\%neg} \geq 20\%$ resulting in a sensitivity of 89% and specificity of 86% (area under the curve AUC = 0.923) for a negative PSMA-PET scan (Fig. 5).

Applying this cutoff ($PSMA_{\%neg} \geq 20\%$) revealed a significant association with lower SUV_{max} values (mean SUV_{max} 17.9 ± 10.9 vs. 6.45 ± 3.7, $p<0.01$, Mann-Whitney U test; Fig. 6A). Eight of nine patients with negative scans had tumours with $PSMA_{\%neg} \geq 20\%$ (89% sensitivity). On the other hand 42 of 49 cases with a $PSMA_{\%neg} < 20\%$ showed a positive PSMA-PET scan (86% specificity). Infiltrative versus expansive growth patterns showed a significant difference in mean SUV_{max}, with expansive tumours having a higher tracer accumulation (mean SUV_{max} 10.0 ± 6.03 vs. 19.9 ± 12.3, $p<0.01$, Mann-Whitney U test) (Fig. 6B). For WHO/ISUP grade groups a significant difference in SUV_{max} values was observed between group 2 and groups 3 to 5 ($p=0.036$, $p=0.005$ and $p=0.001$, Kruskal–Wallis test) and between group 3 and 5 ($p=0.028$, Kruskal–Wallis test) (Fig. 6C). No significant association between cytoplasmic and membranous PSMA IHC expression and SUV_{max} ($p=0.11$, Kruskal–Wallis test and $p=0.13$, Mann-Whitney U test) was found (Fig. 6D+E). In tumours, which expressed PSMA diffusely (100% positive),

homogeneous vs. heterogeneous expression was not associated with significantly different SUV_{max} values (p=0.41, Mann-Whitney U test). A correlation between WHO/ISUP grade groups and $PSMA_{\%neg}$ did not reach significance but showed a trend towards lower grade groups associated with higher percentages of PSMA negative areas (p=0.081, Kruskal–Wallis test). Tumour area and maximum tumour diameter showed a significant positive correlation to higher SUV_{max} values (r=0.426, p=0.001; r=0.318, p=0.015; Pearson's correlation) (Fig. 6F+G).

$PSMA_{\%neg}$, growth pattern, WHO/ISUP grade groups, cytosolic and membranous PSMA expression were selected as variables for the multiple logistic regression analysis (characteristics of the univariable logistic regression analyses are listed in the supplements). None of the selected variables did show a relevant multicolinearity (VIF < 5). The multiple logistic regression model revealed $PSMA_{\%neg}$ (p<0.01, OR=9.629) and growth pattern (p=0.0497, OR=306.537) as independent predictors for a negative PSMA-PET scan. Tab. 2 lists the characteristics of the multiple logistic regression model.

Table 2

Results of a multiple logistic regression model to predict negative PSMA-PET scans.

Variable	Estimate (log odds)	SE	p-value	OR	95% CI OR
Intercept	4.657	4.532	0.304	105.279	0.015 - 758328.777
PSMAneg% (per 20% change)	2.265	0.043	0.008	9.629	8.854 - 10.471
Infiltrative growth pattern	5.725	2.917	0.0497	306.537	1.007 - 93274.818
ISUP	-2.132	1.205	0.077	0.119	0.011 - 1.258
PSMAcytosol	-1.345	1.650	0.415	0.261	0.01 - 6.608
PSMAmembr	-1.581	2.225	0.477	0.206	0.003 - 16.116
CI = confidence interval; OR = odds ratio; PSMAcyto = PSMA expression in the cytosol; PSMAmembr = PSMA expression on the membrane; $PSMA_{\%neg}$ = PSMA-negative tumour area; SE = standard error					

Discussion

In the present study, we correlated ^{68}Ga-PSMA-11-PET results with immunohistochemical PSMA expression patterns as well as histopathological features in prostate carcinomas of 58 RPE specimen using a precise colocalization approach. Significantly lower SUV_{max} values were found in PSMA-PET of prostate carcinoma with $PSMA_{\%neg}$, infiltrative growth pattern, smaller tumour size and WHO/ISUP grade group 2. No significant differences in SUV_{max} could be observed regarding cytoplasmic and membranous PSMA IHC expression intensity levels.

Direct correlation of ^{68}Ga-PSMA-11-PET uptake with immunohistochemical PSMA expression in RPE specimen has been described only by Woythal et al. They demonstrated a significantly lower SUV_{max} in PCa RPE specimen (n=31) which showed an immunoreactive score (IRS) smaller than 2 or a PSMA staining in less than 50% of the tumour cells (20). In our analysis, we also confirmed significantly lower SUV_{max} values in PCa showing PSMA negative areas (ranging from 5% to 80%) (Fig. 7 A+B). In a ROC curve analysis we determined an optimal cutoff value of ≥ 20% $PSMA_{\%neg}$ yielding the highest sensitivity and specificity for a negative PSMA-PET (defined as SUV_{max} <5). In terms of PSMA intensity, we scored the cytoplasmic and membranous PSMA expression separately instead of using a score where cytoplasmic and membranous expression is evaluated simutanously (e.g. the IRS). Interestingly, we found only a positive trend of cytoplasmic (p=0.11, Kruskal–Wallis test) and membranous (p=0.13, Mann-Whitney U test) PSMA expression levels correlating with PSMA-PET positivity, which did not reach statistical significance.

Although different parameters correlated with PSMA-PET negativity, $PSMA_{\%neg}$ and infiltrative growth pattern was found to predict negative PSMA-PET scans in a multiple logistic regression model. This is in concordance with another recently published paper of our group describing $PSMA_{\%neg}$ as a parameter able to predict negative PSMA-PET scans in a biochemical recurrence setting (27). The selection of an absolute cutoff for negative and positive scans is controversial, we therefore selected values with SUV_{max} ≥ 5 for the manuscript, and SUV_{max} ≥ 4 in the supplements, both yielding $PSMA_{\%neg}$ ≥ 20% as the optimal cutoff for negative versus positive scans (Supplements).

The investigation of histopathological parameters, such as the growth pattern of the prostate cancer lesion (detached from conventional grading) in exact correspondence to PSMA-PET has not been published yet. We defined an infiltrative growth as entrapped benign glands within the carcinoma complexes whereas an expansive growth pattern showed pure carcinoma glands within an area of at least 3 circles 5 mm^2 of each (radius 1.26 mm). In an infiltrative growth pattern the density of tumour complexes is decreased by intermingled benign glands. As Woythal et al. stated, benign glands not only show lower PSMA expression but also have a significant lower SUV_{max} in the PSMA-PET than prostate carcinoma (20). Multiple logistic regression also reached statistical significance for infiltrative growth pattern predicting a negative PET scan (p=0.0497).

We decided to exclude all (n=4) very small prostate carcinomas (diameter < 5 mm) because of a natural resolution limit of PSMA-PET scans due to partial-volume effects (23). Woythal et al. stated no correlation between mean tumor size and SUV_{max}. Instead, in this study, a significant correlation between tumour size and SUV_{max} values could be observed. Most likely, this can be explained by different measurement methods. Instead of using the tumour size documented in the pathology report we measured maximum diameter and area of each dominant tumour lesion on one slide and precisely compared this to PSMA-PET uptake of the corresponding area.

We detected a significant correlation between lower WHO/ISUP grade groups and lower SUV_{max} values. This is well in line with the current literatur (3-5). Additionally, a trend towards higher percentages of PSMA IHC negative tumour areas and lower WHO/ISUP grade groups could be shown.

Looking at deviating cases, the maximum diameter and growth pattern seems to be influential parameters. Only one case with a PSMA negative area < 20% (1 of 43, 2.3%) revealed a SUV_{max} value of 4 (cutoff for a negative PET SUV_{max} < 5). This tumour had a relatively small diameter of 8.7 mm (overall mean 13.9 mm) and showed an infiltrative growth pattern (Fig. 7C). On the other hand three cases with PSMA negative areas of more than 20%, showed high SUV_{max} values of 11, 13.2 and 13.7. All of these cases revealed a relatively large diameter with a mean of 20.1 mm (overall mean 13.9 mm). Moreover, two of them showed an expansive growth pattern (Fig. 7D).

Our study faces some limitations, including its retrospective and single-center approach. Furthermore, even in our relatively large cohort consisting of 62 RPEs, the number of cases with a high ratio of negative PSMA areas was limited (15 cases $PSMA_{\%neg} \geq 20\%$ and 6 cases with $PSMA_{\%neg} \geq 50\%$) due to the known natural low frequency of PSMA-negative tumours, of around 10% of all PCa. The low number of negative PSMA-PET scans (9 cases) limited the multiple logistic regression analyisis.

This study describes histopathological parameters and immunohistochemical PSMA expression patterns influencing PSMA-PET uptake in RPE specimen. These parameters can be considered as the foundation for potential future biomarkers for PSMA-PET interpretation in prostate cancer. For routine clinical application in a staging setting these findings need to be transferred to core needle biopsies taken before RPE.

Conclusion

This study describe immunhistochemical PSMA negative tumour area, infiltrative growth pattern, smaller tumour size and WHO/ISUP grade group 2 as parameters associated with lower PSMA-PET uptake in RPE specimen of primary prostate cancers. Particularly, 20% or more $PSMA_{\%neg}$ showed the strongest association with negative PET scans. Assessment of histopathological parameters and PSMA expression may serve as the basis of future biopsy-based biomarker development for an individualized imaging approach.

Declarations

1. O'Keefe DS, Su SL, Bacich DJ, Horiguchi Y, Luo Y, Powell CT, et al. Mapping, genomic organization and promoter analysis of the human prostate-specific membrane antigen gene. Biochim Biophys Acta. 1998;1443(1-2):113-27.
2. Mhawech-Fauceglia P, Zhang S, Terracciano L, Sauter G, Chadhuri A, Herrmann FR, et al. Prostate-specific membrane antigen (PSMA) protein expression in normal and neoplastic tissues and its

sensitivity and specificity in prostate adenocarcinoma: an immunohistochemical study using mutiple tumour tissue microarray technique. Histopathology. 2007;50(4):472-83.

3. Perner S, Hofer MD, Kim R, Shah RB, Li H, Moller P, et al. Prostate-specific membrane antigen expression as a predictor of prostate cancer progression. Hum Pathol. 2007;38(5):696-701.
4. Ross JS, Sheehan CE, Fisher HA, Kaufman RP, Jr., Kaur P, Gray K, et al. Correlation of primary tumor prostate-specific membrane antigen expression with disease recurrence in prostate cancer. Clin Cancer Res. 2003;9(17):6357-62.
5. Hupe MC, Philippi C, Roth D, Kumpers C, Ribbat-Idel J, Becker F, et al. Expression of Prostate-Specific Membrane Antigen (PSMA) on Biopsies Is an Independent Risk Stratifier of Prostate Cancer Patients at Time of Initial Diagnosis. Front Oncol. 2018;8:623.
6. Kranzbuhler B, Muller J, Becker AS, Garcia Schuler HI, Muehlematter U, Fankhauser CD, et al. Detection Rate and Localization of Prostate Cancer Recurrence Using (68)Ga-PSMA-11 PET/MRI in Patients with Low PSA Values </= 0.5 ng/mL. J Nucl Med. 2020;61(2):194-201.
7. Burger IA, Muller J, Donati OF, Ferraro DA, Messerli M, Kranzbuhler B, et al. (68)Ga-PSMA-11 PET/MR Detects Local Recurrence Occult on mpMRI in Prostate Cancer Patients After HIFU. J Nucl Med. 2019;60(8):1118-23.
8. Hofman MS, Lawrentschuk N, Francis RJ, Tang C, Vela I, Thomas P, et al. Prostate-specific membrane antigen PET-CT in patients with high-risk prostate cancer before curative-intent surgery or radiotherapy (proPSMA): a prospective, randomised, multicentre study. Lancet. 2020;395(10231):1208-16.
9. Muehlematter UJ, Burger IA, Becker AS, Schawkat K, Hotker AM, Reiner CS, et al. Diagnostic Accuracy of Multiparametric MRI versus (68)Ga-PSMA-11 PET/MRI for Extracapsular Extension and Seminal Vesicle Invasion in Patients with Prostate Cancer. Radiology. 2019;293(2):350-8.
10. Woo S, Ghafoor S, Becker AS, Han S, Wibmer AG, Hricak H, et al. Prostate-specific membrane antigen positron emission tomography (PSMA-PET) for local staging of prostate cancer: a systematic review and meta-analysis. European Journal of Hybrid Imaging. 2020;4(1):16.
11. Eiber M, Weirich G, Holzapfel K, Souvatzoglou M, Haller B, Rauscher I, et al. Simultaneous (68)Ga-PSMA HBED-CC PET/MRI Improves the Localization of Primary Prostate Cancer. Eur Urol. 2016;70(5):829-36.
12. Park SY, Zacharias C, Harrison C, Fan RE, Kunder C, Hatami N, et al. Gallium 68 PSMA-11 PET/MR Imaging in Patients with Intermediate- or High-Risk Prostate Cancer. Radiology. 2018;288(2):495-505.
13. Maurer T, Gschwend JE, Rauscher I, Souvatzoglou M, Haller B, Weirich G, et al. Diagnostic Efficacy of (68)Gallium-PSMA Positron Emission Tomography Compared to Conventional Imaging for Lymph Node Staging of 130 Consecutive Patients with Intermediate to High Risk Prostate Cancer. J Urol. 2016;195(5):1436-43.
14. Yaxley JW, Raveenthiran S, Nouhaud FX, Samaratunga H, Yaxley WJ, Coughlin G, et al. Risk of metastatic disease on (68) gallium-prostate-specific membrane antigen positron emission

tomography/computed tomography scan for primary staging of 1253 men at the diagnosis of prostate cancer. BJU Int. 2019;124(3):401-7.

15. Muehlematter UJ, Rupp NJ, Mueller J, Eberli D, Burger IA. 68Ga-PSMA PET/MR-Positive, Histopathology-Proven Prostate Cancer in a Patient With Negative Multiparametric Prostate MRI. Clin Nucl Med. 2018;43(8):e282-e4.
16. Mannweiler S, Amersdorfer P, Trajanoski S, Terrett JA, King D, Mehes G. Heterogeneity of prostate-specific membrane antigen (PSMA) expression in prostate carcinoma with distant metastasis. Pathol Oncol Res. 2009;15(2):167-72.
17. Paschalis A, Sheehan B, Riisnaes R, Rodrigues DN, Gurel B, Bertan C, et al. Prostate-specific Membrane Antigen Heterogeneity and DNA Repair Defects in Prostate Cancer. Eur Urol. 2019;76(4):469-78.
18. Pizzuto DA, Muller J, Muhlematter U, Rupp NJ, Topfer A, Mortezavi A, et al. The central zone has increased (68)Ga-PSMA-11 uptake: "Mickey Mouse ears" can be hot on (68)Ga-PSMA-11 PET. Eur J Nucl Med Mol Imaging. 2018;45(8):1335-43.
19. Ferraro DA, Rupp NJ, Donati OF, Messerli M, Eberli D, Burger IA. 68Ga-PSMA-11 PET/MR Can Be False Positive in Normal Prostatic Tissue. Clin Nucl Med. 2019;44(4):e291-e3.
20. Woythal N, Arsenic R, Kempkensteffen C, Miller K, Janssen JC, Huang K, et al. Immunohistochemical Validation of PSMA Expression Measured by (68)Ga-PSMA PET/CT in Primary Prostate Cancer. J Nucl Med. 2018;59(2):238-43.
21. Moch H, Cubilla AL, Humphrey PA, Reuter VE, Ulbright TM. The 2016 WHO Classification of Tumours of the Urinary System and Male Genital Organs-Part A: Renal, Penile, and Testicular Tumours. Eur Urol. 2016;70(1):93-105.
22. Epstein JI, Egevad L, Amin MB, Delahunt B, Srigley JR, Humphrey PA, et al. The 2014 International Society of Urological Pathology (ISUP) Consensus Conference on Gleason Grading of Prostatic Carcinoma: Definition of Grading Patterns and Proposal for a New Grading System. Am J Surg Pathol. 2016;40(2):244-52.
23. Soret M, Bacharach SL, Buvat I. Partial-volume effect in PET tumor imaging. J Nucl Med. 2007;48(6):932-45.
24. Rupp NJ, Umbricht CA, Pizzuto DA, Lenggenhager D, Topfer A, Muller J, et al. First Clinicopathologic Evidence of a Non-PSMA-Related Uptake Mechanism for (68)Ga-PSMA-11 in Salivary Glands. J Nucl Med. 2019;60(9):1270-6.
25. Fendler WP, Eiber M, Beheshti M, Bomanji J, Ceci F, Cho S, et al. Ga-68-PSMA PET/CT: Joint EANM and SNMMI procedure guideline for prostate cancer imaging: version 1.0. Eur J Nucl Med Mol I. 2017;44(6):1014-24.
26. Demirci E, Kabasakal L, Sahin OE, Akgun E, Gultekin MH, Doganca T, et al. Can SUVmax values of Ga-68-PSMA PET/CT scan predict the clinically significant prostate cancer? Nucl Med Commun. 2019;40(1):86-91.

27. Ferraro DA, Ruschoff JH, Muehlematter UJ, Kranzbuhler B, Muller J, Messerli M, et al. Immunohistochemical PSMA expression patterns of primary prostate cancer tissue are associated with the detection rate of biochemical recurrence with (68)Ga-PSMA-11-PET. Theranostics. 2020;10(14):6082-94.

References

1. O'Keefe DS, Su SL, Bacich DJ, Horiguchi Y, Luo Y, Powell CT, et al. Mapping, genomic organization and promoter analysis of the human prostate-specific membrane antigen gene. Biochim Biophys Acta. 1998;1443(1–2):113–27.
2. Mhawech-Fauceglia P, Zhang S, Terracciano L, Sauter G, Chadhuri A, Herrmann FR, et al. Prostate-specific membrane antigen (PSMA) protein expression in normal and neoplastic tissues and its sensitivity and specificity in prostate adenocarcinoma: an immunohistochemical study using mutiple tumour tissue microarray technique. Histopathology. 2007;50(4):472–83.
3. Perner S, Hofer MD, Kim R, Shah RB, Li H, Moller P, et al. Prostate-specific membrane antigen expression as a predictor of prostate cancer progression. Hum Pathol. 2007;38(5):696–701.
4. Ross JS, Sheehan CE, Fisher HA, Kaufman RP Jr, Kaur P, Gray K, et al. Correlation of primary tumor prostate-specific membrane antigen expression with disease recurrence in prostate cancer. Clin Cancer Res. 2003;9(17):6357–62.
5. Hupe MC, Philippi C, Roth D, Kumpers C, Ribbat-Idel J, Becker F, et al. Expression of Prostate-Specific Membrane Antigen (PSMA) on Biopsies Is an Independent Risk Stratifier of Prostate Cancer Patients at Time of Initial Diagnosis. Front Oncol. 2018;8:623.
6. Kranzbuhler B, Muller J, Becker AS, Garcia Schuler HI, Muehlematter U, Fankhauser CD, et al. Detection Rate and Localization of Prostate Cancer Recurrence Using (68)Ga-PSMA-11 PET/MRI in Patients with Low PSA Values </= 0.5 ng/mL. J Nucl Med. 2020;61(2):194–201.
7. Burger IA, Muller J, Donati OF, Ferraro DA, Messerli M, Kranzbuhler B, et al. (68)Ga-PSMA-11 PET/MR Detects Local Recurrence Occult on mpMRI in Prostate Cancer Patients After HIFU. J Nucl Med. 2019;60(8):1118–23.
8. Hofman MS, Lawrentschuk N, Francis RJ, Tang C, Vela I, Thomas P, et al. Prostate-specific membrane antigen PET-CT in patients with high-risk prostate cancer before curative-intent surgery or radiotherapy (proPSMA): a prospective, randomised, multicentre study. Lancet. 2020;395(10231):1208–16.
9. Muehlematter UJ, Burger IA, Becker AS, Schawkat K, Hotker AM, Reiner CS, et al. Diagnostic Accuracy of Multiparametric MRI versus (68)Ga-PSMA-11 PET/MRI for Extracapsular Extension and Seminal Vesicle Invasion in Patients with Prostate Cancer. Radiology. 2019;293(2):350–8.
10. Woo S, Ghafoor S, Becker AS, Han S, Wibmer AG, Hricak H, et al. Prostate-specific membrane antigen positron emission tomography (PSMA-PET) for local staging of prostate cancer: a systematic review and meta-analysis. European Journal of Hybrid Imaging. 2020;4(1):16.

11. Eiber M, Weirich G, Holzapfel K, Souvatzoglou M, Haller B, Rauscher I, et al. Simultaneous (68)Ga-PSMA HBED-CC PET/MRI Improves the Localization of Primary Prostate Cancer. Eur Urol. 2016;70(5):829–36.
12. Park SY, Zacharias C, Harrison C, Fan RE, Kunder C, Hatami N, et al. Gallium 68 PSMA-11 PET/MR Imaging in Patients with Intermediate- or High-Risk Prostate Cancer. Radiology. 2018;288(2):495–505.
13. Maurer T, Gschwend JE, Rauscher I, Souvatzoglou M, Haller B, Weirich G, et al. Diagnostic Efficacy of (68)Gallium-PSMA Positron Emission Tomography Compared to Conventional Imaging for Lymph Node Staging of 130 Consecutive Patients with Intermediate to High Risk Prostate Cancer. J Urol. 2016;195(5):1436–43.
14. Yaxley JW, Raveenthiran S, Nouhaud FX, Samaratunga H, Yaxley WJ, Coughlin G, et al. Risk of metastatic disease on (68) gallium-prostate-specific membrane antigen positron emission tomography/computed tomography scan for primary staging of 1253 men at the diagnosis of prostate cancer. BJU Int. 2019;124(3):401–7.
15. Muehlematter UJ, Rupp NJ, Mueller J, Eberli D, Burger IA. 68Ga-PSMA PET/MR-Positive, Histopathology-Proven Prostate Cancer in a Patient With Negative Multiparametric Prostate MRI. Clin Nucl Med. 2018;43(8):e282-e4.
16. Mannweiler S, Amersdorfer P, Trajanoski S, Terrett JA, King D, Mehes G. Heterogeneity of prostate-specific membrane antigen (PSMA) expression in prostate carcinoma with distant metastasis. Pathol Oncol Res. 2009;15(2):167–72.
17. Paschalis A, Sheehan B, Riisnaes R, Rodrigues DN, Gurel B, Bertan C, et al. Prostate-specific Membrane Antigen Heterogeneity and DNA Repair Defects in Prostate Cancer. Eur Urol. 2019;76(4):469–78.
18. Pizzuto DA, Muller J, Muhlematter U, Rupp NJ, Topfer A, Mortezavi A, et al. The central zone has increased (68)Ga-PSMA-11 uptake: "Mickey Mouse ears" can be hot on (68)Ga-PSMA-11 PET. Eur J Nucl Med Mol Imaging. 2018;45(8):1335–43.
19. Ferraro DA, Rupp NJ, Donati OF, Messerli M, Eberli D, Burger IA. 68Ga-PSMA-11 PET/MR Can Be False Positive in Normal Prostatic Tissue. Clin Nucl Med. 2019;44(4):e291-e3.
20. Woythal N, Arsenic R, Kempkensteffen C, Miller K, Janssen JC, Huang K, et al. Immunohistochemical Validation of PSMA Expression Measured by (68)Ga-PSMA PET/CT in Primary Prostate Cancer. J Nucl Med. 2018;59(2):238–43.
21. Moch H, Cubilla AL, Humphrey PA, Reuter VE, Ulbright TM. The 2016 WHO Classification of Tumours of the Urinary System and Male Genital Organs-Part A: Renal, Penile, and Testicular Tumours. Eur Urol. 2016;70(1):93–105.
22. Epstein JI, Egevad L, Amin MB, Delahunt B, Srigley JR, Humphrey PA, et al. The 2014 International Society of Urological Pathology (ISUP) Consensus Conference on Gleason Grading of Prostatic Carcinoma: Definition of Grading Patterns and Proposal for a New Grading System. Am J Surg Pathol. 2016;40(2):244 – 52.

23. Soret M, Bacharach SL, Buvat I. Partial-volume effect in PET tumor imaging. J Nucl Med. 2007;48(6):932–45.
24. Rupp NJ, Umbricht CA, Pizzuto DA, Lenggenhager D, Topfer A, Muller J, et al. First Clinicopathologic Evidence of a Non-PSMA-Related Uptake Mechanism for (68)Ga-PSMA-11 in Salivary Glands. J Nucl Med. 2019;60(9):1270–6.
25. Fendler WP, Eiber M, Beheshti M, Bomanji J, Ceci F, Cho S, et al. Ga-68-PSMA PET/CT: Joint EANM and SNMMI procedure guideline for prostate cancer imaging: version 1.0. Eur J Nucl Med Mol I. 2017;44(6):1014–24.
26. Demirci E, Kabasakal L, Sahin OE, Akgun E, Gultekin MH, Doganca T, et al. Can SUVmax values of Ga-68-PSMA PET/CT scan predict the clinically significant prostate cancer? Nucl Med Commun. 2019;40(1):86–91.
27. Ferraro DA, Ruschoff JH, Muehlematter UJ, Kranzbuhler B, Muller J, Messerli M, et al. Immunohistochemical PSMA expression patterns of primary prostate cancer tissue are associated with the detection rate of biochemical recurrence with (68)Ga-PSMA-11-PET. Theranostics. 2020;10(14):6082–94.

Figures

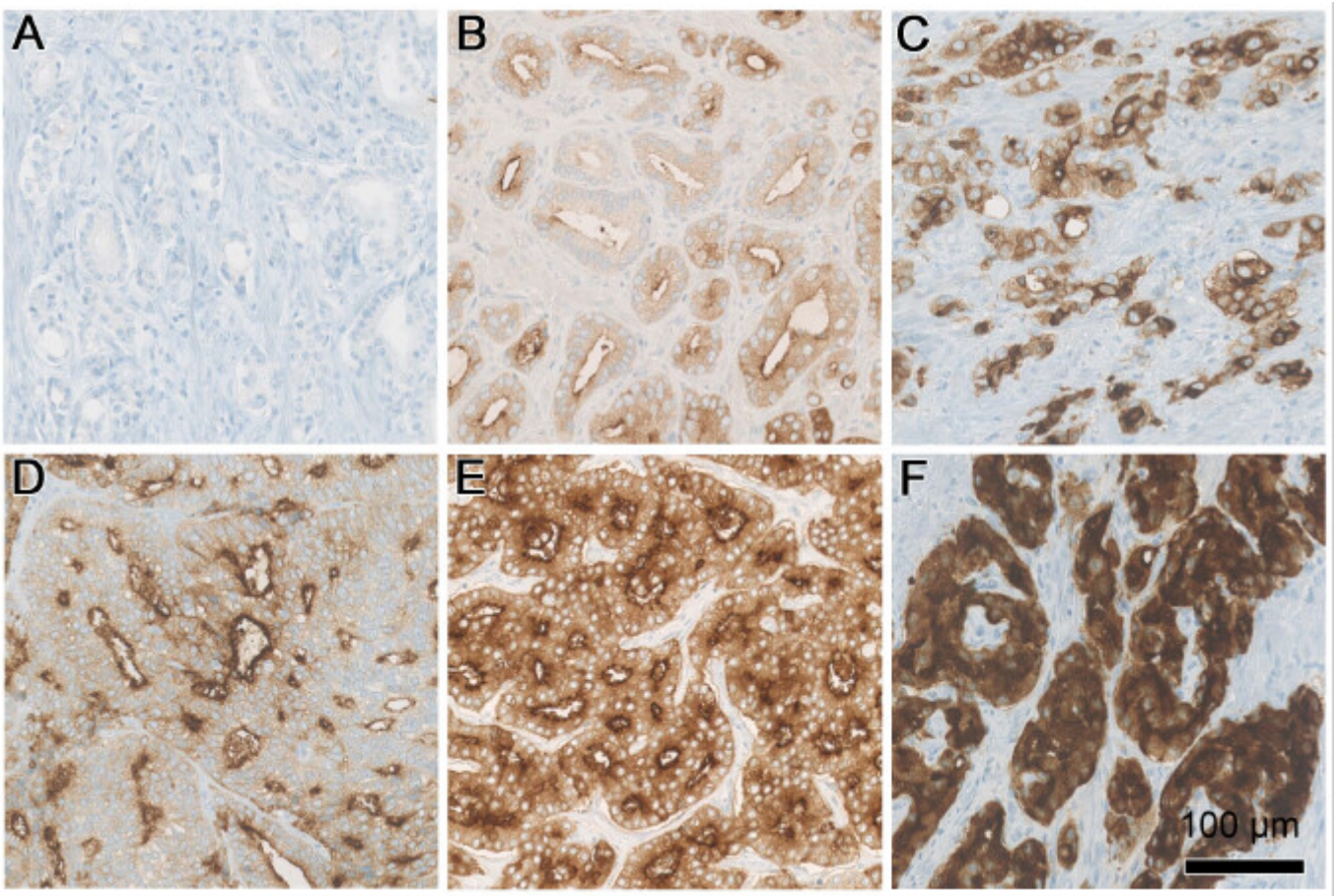

Figure 1

Overview of the different immunohistochemical PSMA staining patterns. (A) shows complete negativity, while (B) depicts low expression of cytoplasmic (1+) and moderate membranous (2+) PSMA staining. In (C) a moderate membranous and cytoplasmic (2+) staining is shown. (D) illustrates low cytoplasmic (1+) and strong membranous (3+) expression. (E) shows moderate (2+) cytoplasmic and strong membranous (3+) expression, while (F) shows diffuse strong (3+) cytoplasmic and membranous expression. Scale bar 100 µm.

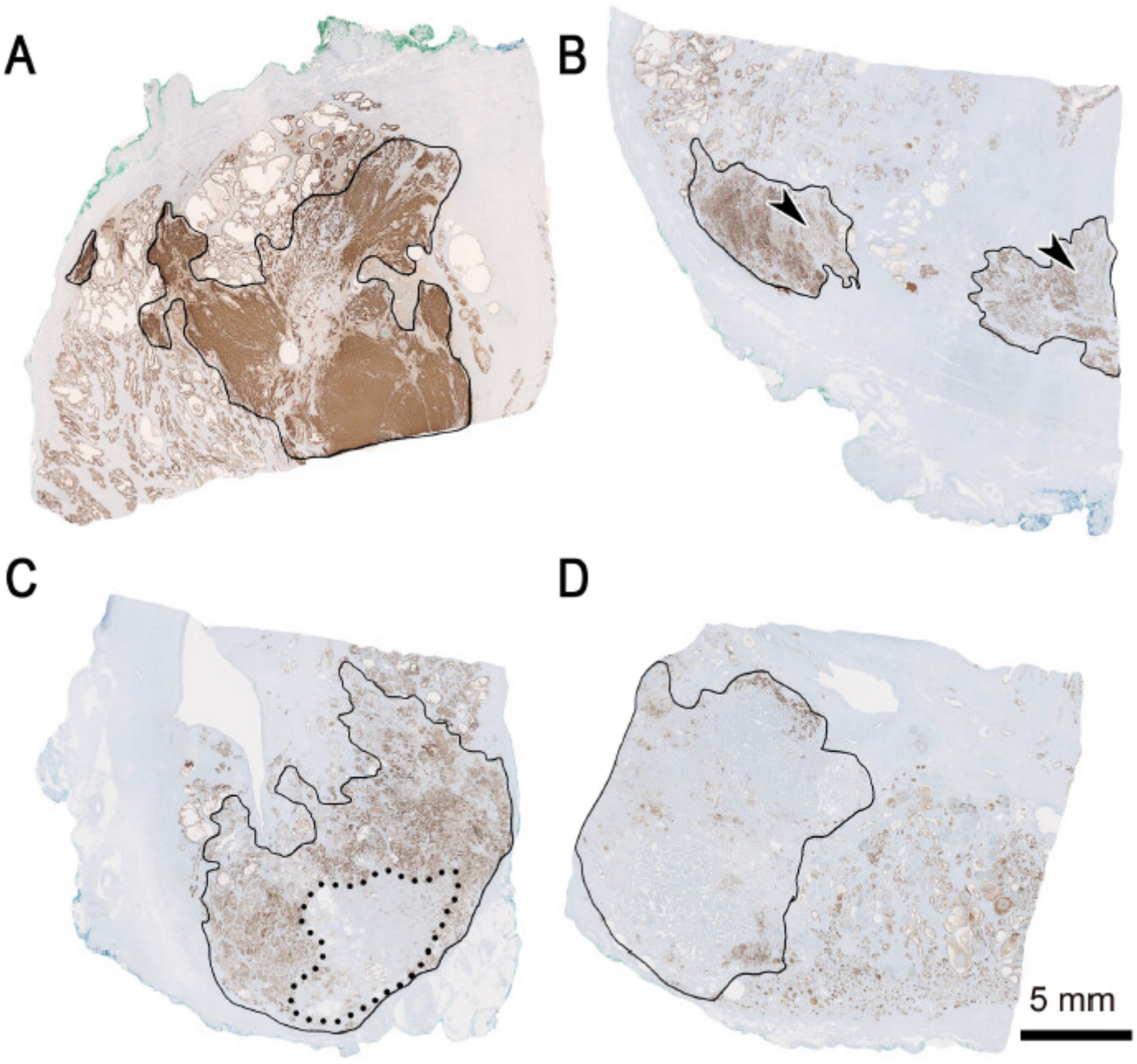

Figure 2

Overview of the different immunohistochemical PSMA heterogeneity patterns. (A) shows homogenous strong and diffuse positivity. (B) depicts heterogenous PSMA positivity with focal weaker expression (arrowheads) in different components of the carcinoma, without negative areas. In (C) the circled

carcinoma (continuous line) consists of approximately 30% (dotted line) negative areas. Whereas in (D) roughly 80% of the marked invasive carcinoma shows negativity. Scale bar 5 mm.

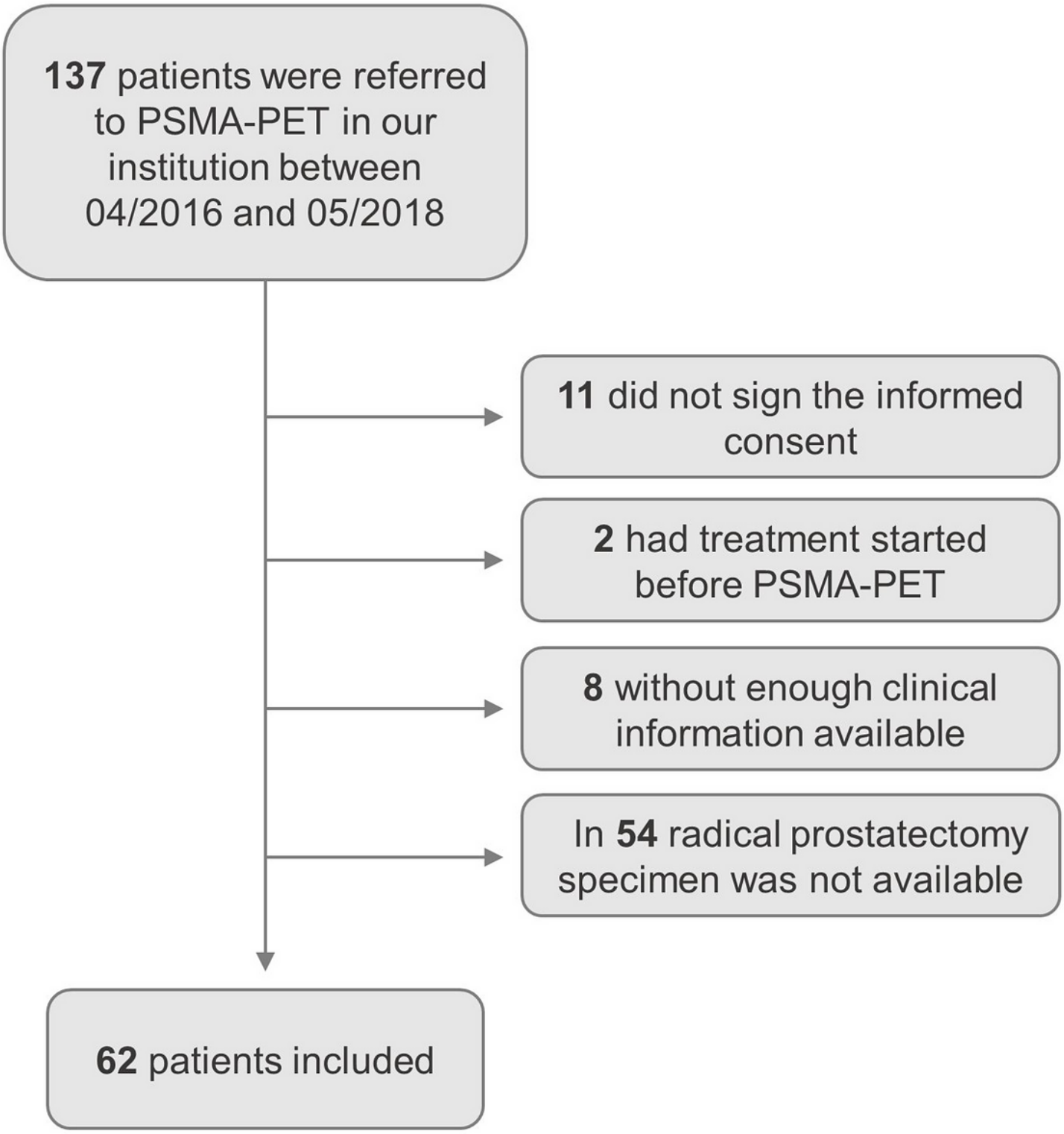

Figure 3

Patient inclusion flowchart.

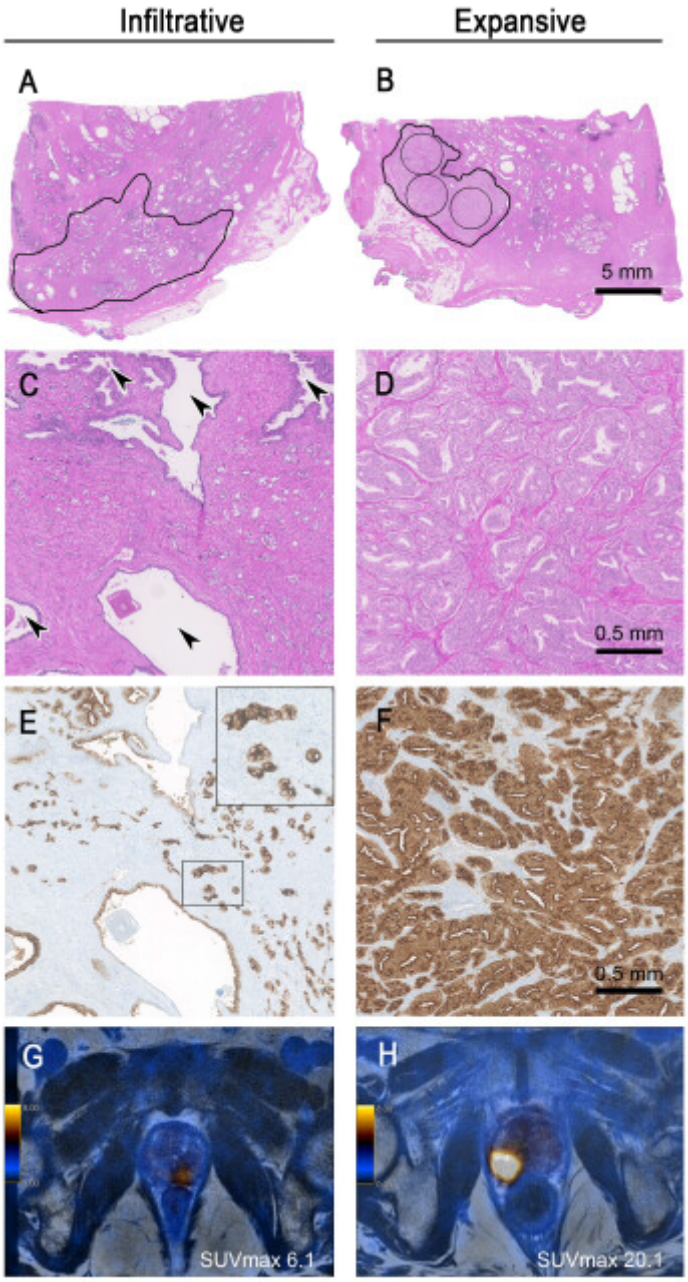

Figure 4

Examples of infiltrative and expansive growth patterns. (A, C) is an example of a prostate carcinoma growing between normal glands (arrowheads in C) refered to as infiltrative growth pattern. (B, D) depicts a prostate carcinoma which homogenously consists of tumour glands comprising at least 3 circles of 5 mm2 each (radius 1.26 mm). This is regarded as expansive growth pattern. While both cases (A, B) have tumour diameters in a similar range(12 mm and 7 mm, respectively), identical Gleason patterns (both 4+4, WHO/ISUP grade group 4) and similar PSMA expression (both cytoplasmic 2+ and membranous 3+) (E, F) the SUVmax values are clearly different (SUVmax 6.1 vs. 20.1) (G, H). (A, B) Scale bar 5 mm, (C, D) Scale bar 0.5 mm.

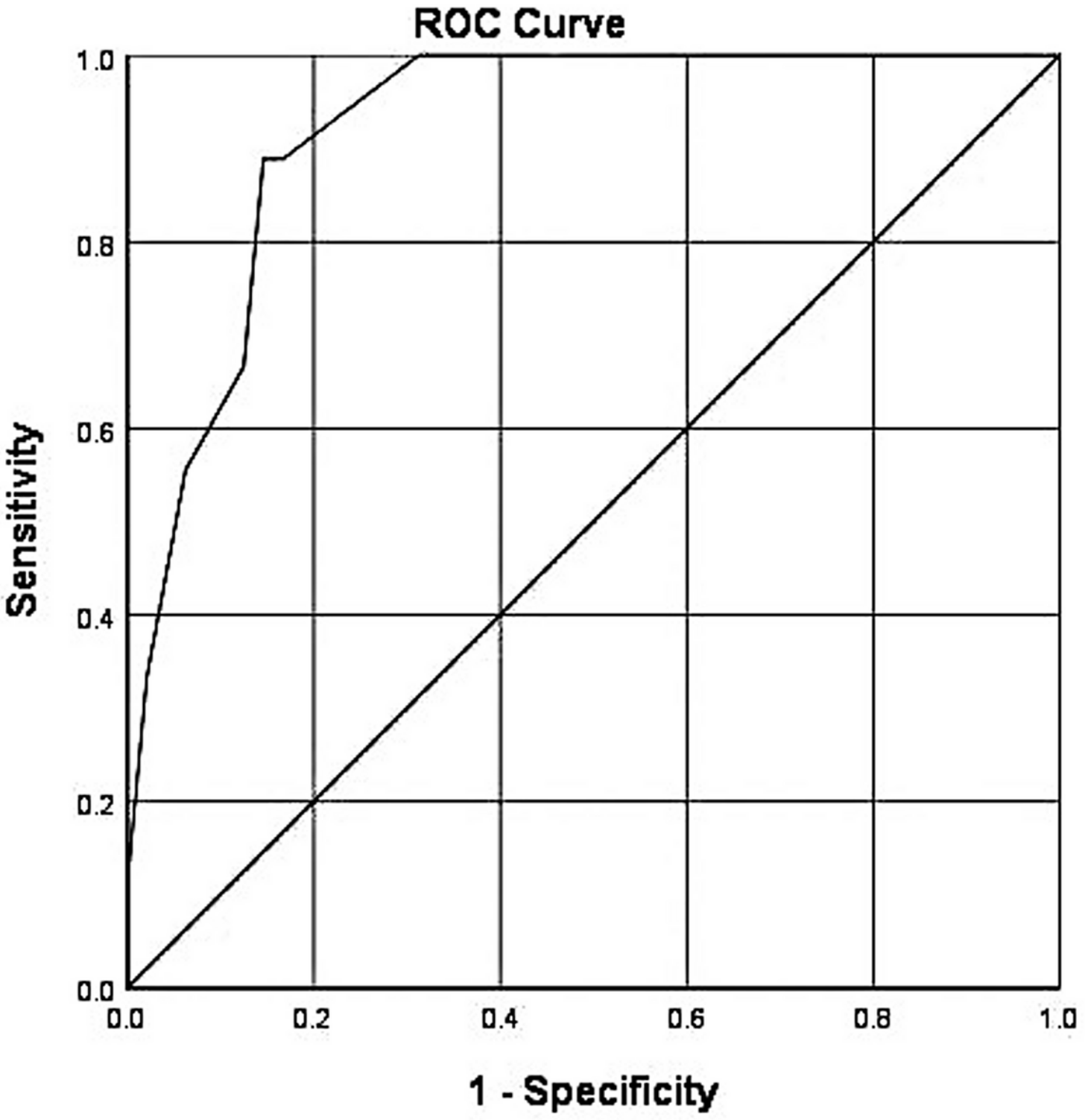

Figure 5

ROC Curve analysis for PSMA%neg and negative PET scan. A cutoff value of 20% PSMA%neg yielded sensitivity of 89% and specificity of 86% (area under curve 0.923) for a negative PSMA-PET scan (defined as SUVmax < 5).

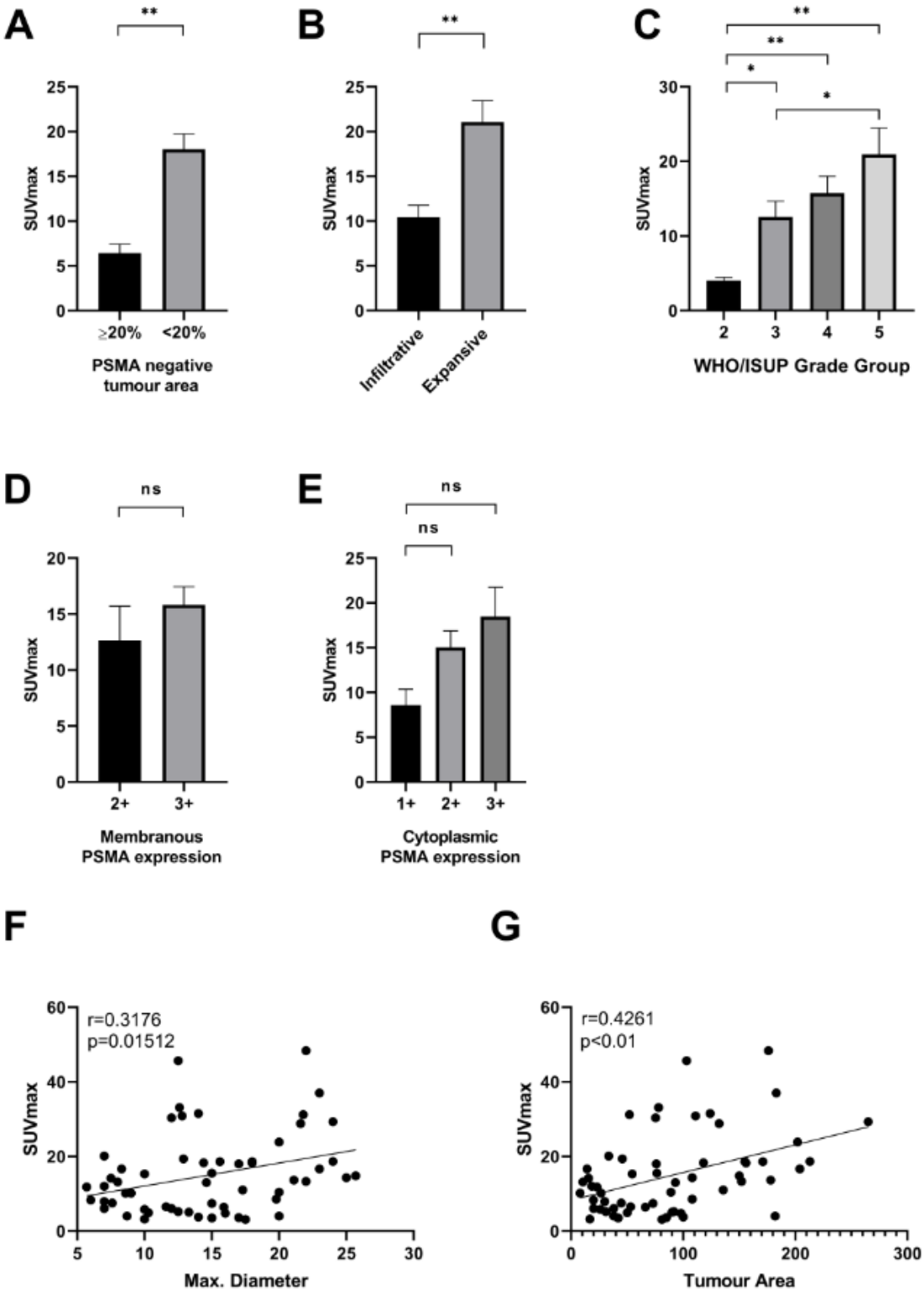

Figure 6

Column plots with standard error of mean (SEM) and scatter plots showing relations between SUVmax values and different tissue characteristics. Significant lower SUVmax values could be found in prostate carcinomas with PSMA IHC negative area (PSMA%neg) ≥ 20% (A), an infiltrative growth pattern (B), WHO/ISUP grade group 2 and 3 (C) but not in carcinomas with low cytoplasmic or membranous PSMA staining intensities (D, E). SUVmax values significantly correlated with maximum tumour diameter

(r=0.318, p=0.015, Pearson's correlation) as well as tumour area (r=0.426, p<0.01, Pearson's correlation) (F, G). * p<0.05, ** p<0.01

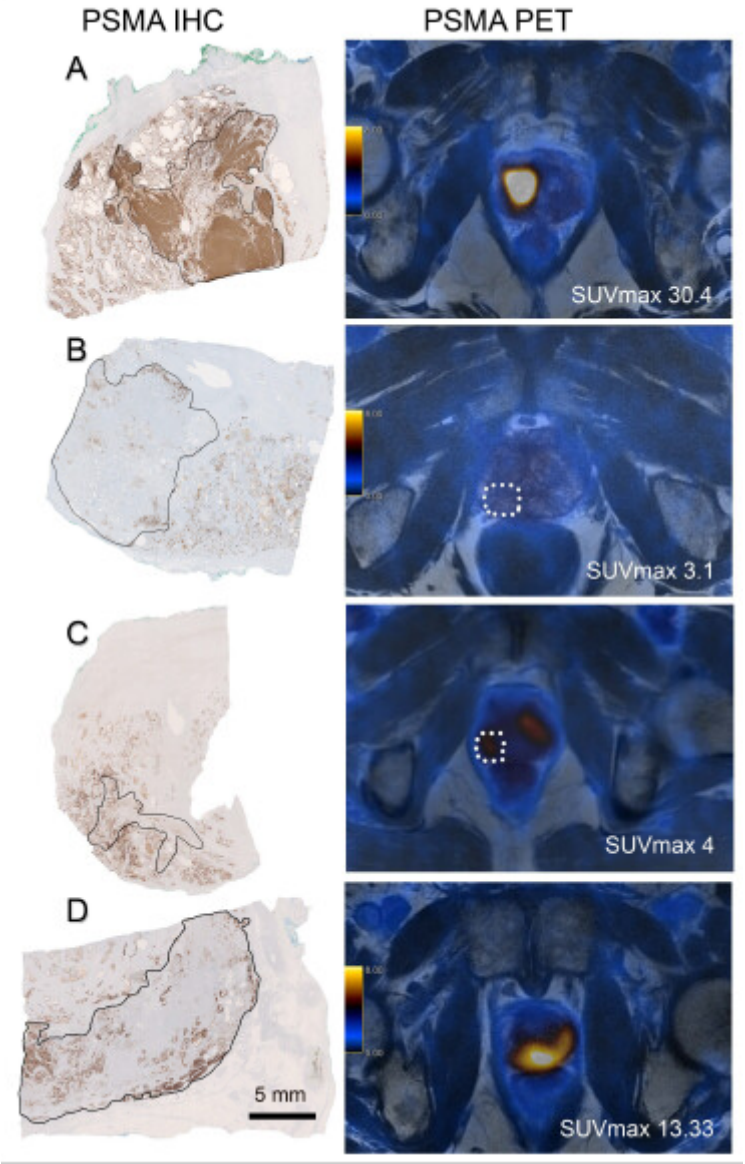

Figure 7

Examples of PSMA expression on immunohistochemistry (IHC) and 68Ga-PSMA-PET results. (A) Illustration of a prostate carcinoma with a strong homogenous PSMA expression (left) and a high SUVmax located in the anterior right part of the gland. (B) Example of a prostate carcinoma (circled) showing almost no PSMA IHC staining (80% negative tumour area) and also lacking PSMA-PET positivity in the corresponding area. (C) is a case that shows a predominantly PSMA IHC positive prostate carcinoma (only 5% completely PSMA negative glands) with a low PSMA-PET positivity (SUVmax 4). Note the small diameter of this carcinomatous focus (8.7 mm). (D) Conversely, this carcinoma with a diameter of 22 mm shows a high PSMA-PET positivity (SUVmax 13.33) despite a heterogenous, largely lacking PSMA IHC expression (almost 70% negative areas). Scale bar 5 mm.

Supplementary Files

This is a list of supplementary files associated with this preprint. Click to download.

- Supplementary.docx